Leaky and bound modes of surface plasmon waveguides

Rashid Zia,* Mark D. Selker, and Mark L. Brongersma

Geballe Laboratory for Advanced Materials, Stanford University, Stanford, California 94305, USA
(Received 5 August 2004; revised manuscript received 7 February 2005; published 26 April 2005)

While theoretical studies of finite width plasmonic waveguides have focused on the bound modal solutions of metallic structures in homogeneous or near-homogeneous dielectric matrices, experimental studies have mainly probed the leaky surface plasmon modes along the air-exposed surfaces of metallic stripes on glass substrates. Combining a full-vectorial, magnetic field finite-difference method with complex coordinate stretching perfectly matched layer boundary conditions, we have solved for both the leaky and bound modes of metallic slab and stripe waveguides. Solutions for the leaky modes excited via attenuated total reflection in the Kretschmann configuration provide added insight into the results of recent near and far-field experimental studies. For these cases, an analytical approximation for the number of allowed modes as a function of waveguide width is derived based upon the guidance condition of dielectric waveguide theory. Then, consistent with a ray optics interpretation for surface plasmon-polariton propagation, a direct comparison is made between our simulations and published results with regard to field profiles and propagation lengths.

I. INTRODUCTION

Surface plasmon polaritons (SPPs) have received much attention in recent years.[1] A great part of this renewed interest concerns the proposed potential of plasmonic waveguides to guide electromagnetic energy at optical frequencies below the diffraction limit.[2–5] Although subwavelength confinement of optical modes has yet to be accomplished, the design of such modes for two-dimensional, metallic slab waveguides has been achieved,[6] and promising experimental results have demonstrated that a 200 nm wide Au stripe can guide 800 nm wavelength light for several microns.[7] Given the fast pace of experimental research in the field,[7–12] and the maturation of numerical methods to treat SPPs,[13–15] it is likely that in the near future highly confined, three-dimensional plasmonic waveguides will be realized.

The best studied three-dimensional plasmonic waveguides to date have been finite width metal stripes, which have been the focus of numerous far-field and near-field characterization studies.[7–12] These structures, usually generated by electron beam lithography, consist of thin patterned Au or Ag stripes mounted on glass substrates.[8] Excitation of metal stripe waveguides has been achieved primarily via attenuated total reflection (ATR) in the Kretschmann configuration.[16] The glass substrates with the deposited metal stripes are optically coupled to a quartz prism by index matching fluid, and far-field light is angled through the prism such that the in-plane wave vector corresponds to the associated surface plasmon propagation constant. It must be noted that if light can couple into the surface plasmon mode through the substrate, light from the surface plasmon mode must be able to couple out through the substrate as well. As shown in Fig. 1, such excitation can efficiently allow mode coupling into leaky surface plasmon modes (i.e., those between the air and glass light lines),[17] but the Kretschmann configuration can never excite purely bound modes (i.e., those to the right of the glass light line).

Despite the dominance of leaky modes in experimental studies, theoretical investigations of metal stripe waveguides

have been limited to bound modes.[13–15] While the bound modal solutions may be excited via end-fire excitation or scattering events,[18] their relevance in characterizing and understanding the behavior of leaky surface plasmon modes excited by ATR has not been validated. Without the benefit of leaky modal solutions, it has been previously suggested that SPPs guided along metal stripes cannot be resolved with the conventional physical models for dielectric waveguides. In this paper, we will introduce a numerical technique that can solve for both the leaky and bound modal solutions of plasmonic waveguides. Then, by simulating the modes of published experimental studies, we will demonstrate that the propagation of surface plasmon modes can be resolved with dielectric waveguide theory.

II. NUMERICAL TECHNIQUE

Recent work has demonstrated that the bound modal solutions of plasmonic waveguides are hybrid TE-TM modes, and therefore, proper analysis requires numerical solution of the full vectorial wave equation.[15] In particular, Al-Bader demonstrated that the full vectorial magnetic field finite difference method (FVH-FDM) outlined in Ref. 19 can success-
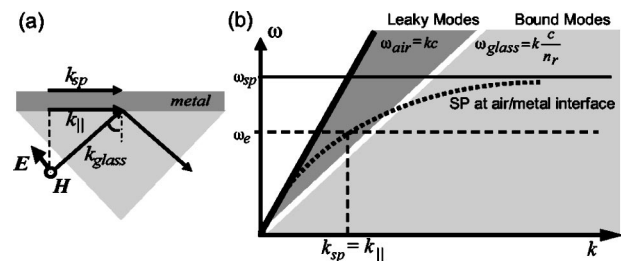

FIG. 1. (a) Schematic view of momentum conservation in Kretschmann Configuration ATR which allows far-field radiation modes in the glass to couple to SPPs at air-metal interface. (b) Dispersion relation for this system which demonstrates that SPPs excited by ATR are leaky modes which can reradiate in the glass.

TABLE I. Comparison of complex propagation constants for AlGaAs/GaAs rib waveguide as calculated by the present FVH-FDM with CCS-PMLs, a FVH imaginary distance finite-element beam propagation method (see Ref. 23), the spectral index method (see Ref. 24), and an edge-based finite-element method with PMLs (see Ref. 25). These quasi-TE modes are labeled according to Ref. 23 by the number of horizontal and vertical extrema planes for the dominant H_y field. (For example, the H^y_{12} mode has one extrema in the x dimension, and two extrema in the y dimension.)

Mode	FVH-FDM w/CCS-PML	FVH-IDFEBPM	SIM	FEM w/PML
H^y_{11}	$3.5738 + i1.6973 \times 10^{-7}$	$3.573733 + i1.693 \times 10^{-7}$	$3.5738 + i1.697 \times 10^{-7}$	$3.573795 + i1.712 \times 10^{-7}$
H^y_{12}	$3.5432 + i5.418 \times 10^{-5}$	$3.543067 + i5.739 \times 10^{-5}$	$3.543231 + i5.481 \times 10^{-5}$	$3.543225 + i5.5691 \times 10^{-5}$
H^y_{13}	$3.4944 + i8.8042 \times 10^{-4}$	$3.493831 + i9.179 \times 10^{-4}$	$3.494279 + i8.841 \times 10^{-4}$	$3.494256 + i8.8313 \times 10^{-4}$

fully solve for the modes of metal stripe waveguides. However, with conventional Dirichlet, Neumann, or Robin boundary conditions, this technique can only solve for bound modes, because these boundaries cannot account for the nonzero radiating fields of leaky modes. Transparent or absorbing boundary conditions (TBCs or ABCs) are required to appropriately treat the semi-infinite extent of leaky modes into a high index substrate. For scalar finite difference methods, it has been shown that perfectly matched layer (PML) ABCs allow for accurate solution of leaky modes in planar waveguides.[20] For our study, we have extended this technique for use with three-dimensional waveguides by implementing the generalized complex coordinate stretching (CCS) formulation of PML boundary conditions.[21] Chew et al. have derived a set of relationships describing electromagnetic waves in complex space that are isomorphic with respect to Maxwell's equation. This formulation has been previously implemented for a similar finite difference method in cylindrical coordinates.[22] Borrowing from the notation in Ref. 22, we have implemented CCS-PML boundary conditions by modifying the relevant Helmholtz equations of the FVH-FDM as follows

$$\frac{\partial^2 H_x}{\partial \tilde{x}^2} + \frac{\partial^2 H_x}{\partial \tilde{y}^2} + \left[\varepsilon \beta_0^2 - (\beta + i\alpha)^2 \right] H_x = 0 \qquad (1)$$

$$\frac{\partial^2 H_y}{\partial \tilde{x}^2} + \frac{\partial^2 H_y}{\partial \tilde{y}^2} + \left[\varepsilon \beta_0^2 - (\beta + i\alpha)^2 \right] H_y = 0 \qquad (2)$$

where $(\beta + i\alpha)$ represents the complex propagation constant, β_0 is the free space wave number, and the complex coordinates $\tilde{x}$ and $\tilde{y}$ are described by substituting x and y for ζ in the following change of variables

$$\tilde{\zeta} = \int_0^\zeta s_\zeta(\zeta') d\zeta' \qquad (3)$$

$$s_\zeta(\zeta) = \begin{cases} 1 + i \dfrac{\sigma_\zeta(\zeta)}{\omega \mu_0}, & \text{within the PML} \\ 1, & \text{elsewhere} \end{cases} \qquad (4)$$

and

$$\sigma_\zeta(\zeta) = \sigma_{\zeta,\max} \left(\frac{\zeta - \zeta_0}{d} \right)^m \qquad (5)$$

In Eqs. (3)–(5), s_ζ is a complex stretching factor, and σ_ζ represents a conductivitylike loss term whose profile in the PML region of thickness d is increasing as an mth order polynomial from a minimum value of zero at the initial PML interface (ζ_0) to a maximum value ($\sigma_{\zeta,\max}$) at the simulation boundary. Rescaling the spatial coordinates of mesh points within the PML region by a complex number allows for attenuation of fields radiating from leaky waveguide modes without the introduction of an impedance mismatch and the associated reflective perturbation of the finite difference solution.

The efficacy of our FVH-FDM code with CCS-PML boundary conditions was validated by comparison with the published modal solutions of numerous two- and three-dimensional waveguides. As a representative example, our solution for the standard leaky GaAs/AlGaAs rib waveguide used in the verification of three-dimensional leaky mode solvers is compared with several published results in Table I.[23] Additionally, to demonstrate applicability and versatility, the leaky surface plasmon mode commonly excited by ATR of a metal thin film was solved by incorporation of periodic boundary conditions for the lateral boundaries of our three-dimensional mode solver. Figure 2 shows the solution for the surface plasmon mode localized at the air-metal interface of a 55 nm thick Au film ($\varepsilon = -26.1437 + 1.8497i$ at $\lambda = 800$ nm)[26] mounted on a fused quartz substrate ($n = 1.46$).
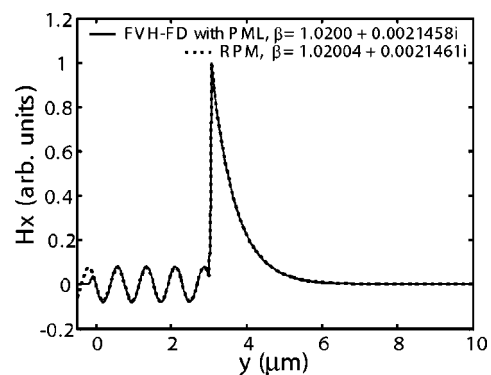

FIG. 2. Transverse magnetic field intensity for the two-dimensional leaky surface plasmon mode as calculated by present FVH-FDM with CCS-PMLs and the RPM.

For this two-dimensional problem, comparison with the well-established reflection pole method (RPM) illustrates the numerical accuracy of this FDM.[27] Note that the field profiles calculated by the two methods are indistinguishable for the waveguiding region; divergence only occurs near to and within the PML region (i.e., $y < 0$) where absorption is introduced for the FDM such that the leakage radiation can be attenuated before reaching the simulation boundary.

III. RESULTS AND DISCUSSION

Recent photon scanning tunneling microscopy (PSTM) experiments have demonstrated the existence of surface plasmon modes along metal stripe waveguides.[11] Varying width Au stripes protruding from an extended thin film region were excited by a modified ATR setup, whereby SPPs launched in the film area propagate through a tapered region to the stripe waveguides. The field intensity profiles across the stripes were then measured by a near-field optical probe, and Weeber *et al.* concluded that bound modes similar to those predicted in Ref. 14 were observed. To investigate these results, we have utilized the aforementioned numerical technique to find both the bound and leaky modal solutions of similar, rectangular cross-section Au stripes mounted on a glass substrate ($n = 1.46$). A variety of modes can be excited along such stripes, including corner and lateral edge modes which have dominant magnetic fields along the vertical axis (H_y). However, we have chosen to focus on those modes localized at the top and bottom metal interfaces which have dominant magnetic fields along the horizontal axis (H_x). Such quasi-TM modes are most likely to be excited by overlap with the pure TM SPPs excited along the extended film region. As an illustrative example, Fig. 3 shows the simulated field components for the two leaky quasi-TM modes supported by a 3.5 μm wide, 55 nm tall Au stripe waveguide, and Fig. 4 shows two of the four bound quasi-TM modes supported by this same structure. From the field intensities, it is clear that the bound modes are localized at the glass-Au interface while the leaky modes are localized at the air-Au interface. Given that the original excitation was achieved by ATR,[11] the SPPs present in the extended film region were necessarily leaky waves, localized at the air-Au interface. Note that these SPPs would have significantly greater overlap with the leaky modes supported by the metal stripe, and one would expect that the leaky stripe modes would be excited much more efficiently than the bound modes. Moreover, the leaky modes have significantly higher field intensities in the air region above the stripe where the near-fields are probed. Therefore, the compound experimental difficulties of exciting and observing the bound stripe modes suggest that the dominant surface plasmon modes observed have been leaky stripe modes. This indeed agrees with experimental observations, as will be discussed later in Sec. III B.

A. Dependence of modal behavior on stripe width

To investigate the propagation of SPPs along metal stripes, we have first performed a parametric numerical study of stripe modes. For a constant waveguide thickness (t) of 55 nm, the modal solutions for a free space wavelength of 800 nm were found as a function of varying waveguide width (W). The complex propagation constants ($\beta + i\alpha$) of the lowest order leaky and bound quasi-TM modes are plotted in Figs. 5 and 6, respectively. Several important trends can be discerned from these plots. First and foremost is the insight that for these structures a cutoff width exists below which no quasi-TM modes are allowed, and that this cutoff width is substantially larger for leaky surface plasmon modes as compared to bound modes (~ 1.3 μm vs ~ 0.6 μm). Second, for increasing stripe widths, higher order modes associated with additional extrema in the H_x field along the stripe width become accessible, while as expected, the propagation constants for the lowest order modes asymptotically approach those associated with two-dimensional SPPs localized at the air-metal and glass-metal dielectric interfaces. Third, for decreasing stripe widths, confinement of the quasi-TM modes within the metal stripe is reduced. For the bound SPP modes, this diminished confinement results in lower losses (i.e., a smaller α), because heating within the metallic region is the sole loss mechanism. Yet, the opposite is true for leaky modes, because increases in radiation losses are more significant than reductions in metallic losses for thin stripes.

These last observations regarding confinement can be used to derive a physical picture for the number of modes supported in a given width strip. Given that the propagation constant along the stripe asymptotically approaches the value along an extended film, it is reasonable to assume that the in-plane momentum for a SPP supported by an infinitely wide metal-dielectric interface (k_{sp}) is conserved for a SPP on a finite width structure. However, along the finite width stripe, this in-plane wave vector can be separated into a component along the direction of propagation (k_z) as well as lateral component (k_x) such that

$$k_x^2 + k_z^2 = k_{sp}^2 \qquad (6)$$

where neglecting finite stripe thickness, the in-plane wave vector (k_{sp}) can be approximated by the following expression for the SPP supported by a simple metal-dielectric interface[16]

$$k_{sp} = \frac{\omega}{c}\sqrt{\frac{\varepsilon_d \varepsilon_m}{\varepsilon_d + \varepsilon_m}} \qquad (7)$$

In Eq. (7), ε_d and ε_m are the relative permittivities in the dielectric and metal regions, respectively.

In order for waveguiding to occur, there is a lower limit placed upon the propagating component of momentum.[28] The guided SPPs should not be able to couple into the radiation modes of the surrounding dielectric material; therefore, the propagating wave vector must exceed the effective wave number within the dielectric region [i.e., $|k_z| > (\omega/c)\sqrt{\varepsilon_d}$]. At this guiding limit, we can easily use Eqs. (6) and (7) to derive the maximum value for the lateral wave vector

$$|k_x| < \left(\frac{\omega}{c}\right)\sqrt{\frac{\varepsilon_d \varepsilon_m}{\varepsilon_d + \varepsilon_m} - \varepsilon_d} \qquad (8)$$

This maximum value for k_x limits quantization along the lateral direction, and thus, we can approximate the number of
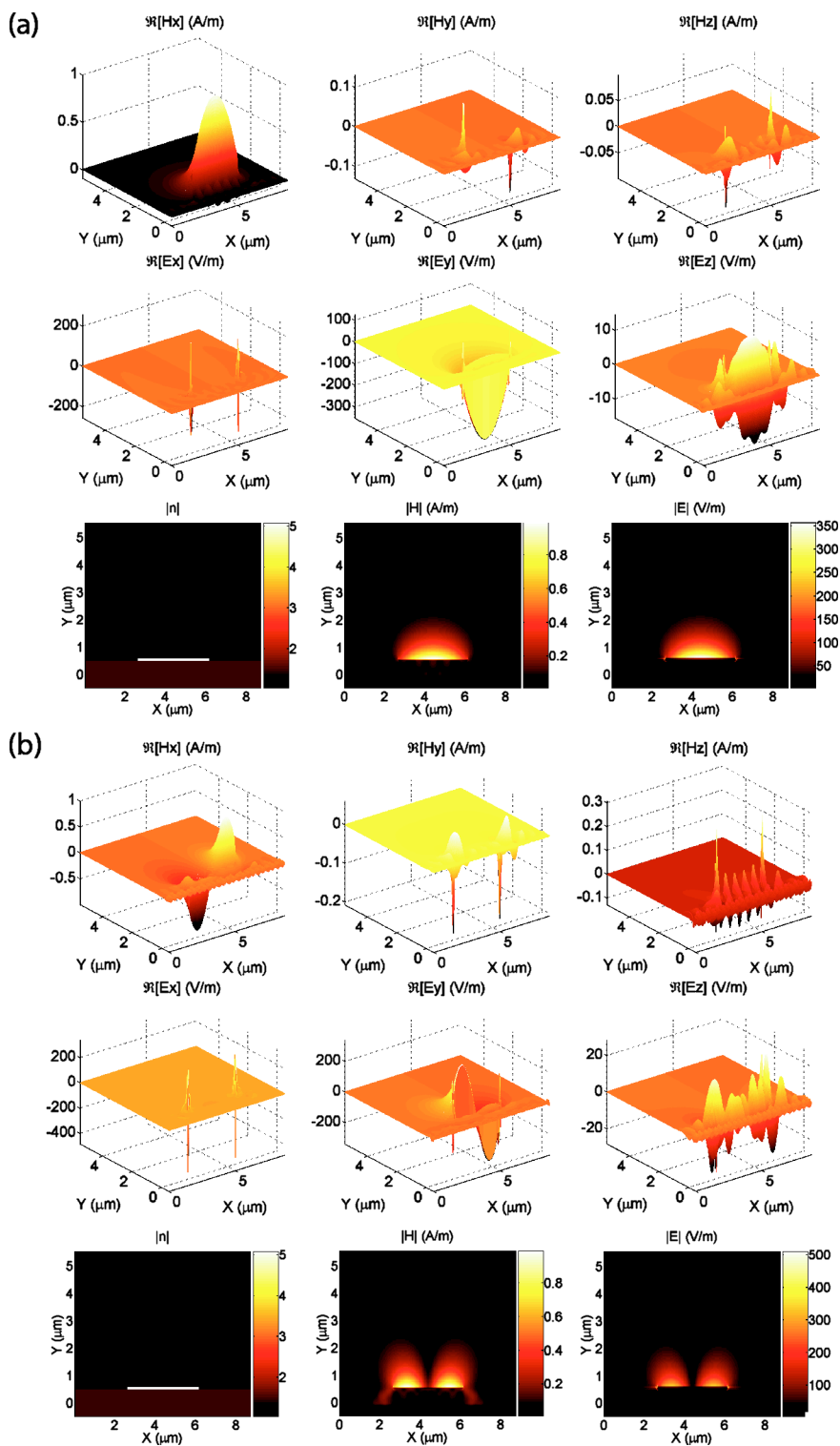
FIG. 3. (Color online) Simulated field profiles for two leaky quasi-TM surface plasmon modes of a 3.5 μm wide, 55 nm tall Au stripe waveguide on glass substrate (λ=800 nm): (a) lowest order leaky mode and (b) second order leaky mode. Note that these leaky modes are localized at top air-metal interface and radiate through the glass substrate into the PML region ($y<0$). (All fields have been normalized such that max$|H_x|$=1 A/m, and the simulated refractive index profile has been provided alongside each mode for reference.)

allowed SPP modes (N) by relating the width (W) of the interface to the lateral wave vector. As the highest order supported mode would have N number of extrema in the lateral direction, the maximum lateral wave vector would be

$$k_{x,\max} = \frac{N\pi}{W} \tag{9}$$

Simplifying Eqs. (8) and (9), we derive an approximate analytical expression for the number of supported modes

$$N < \frac{2W}{\lambda} \sqrt{\frac{-\varepsilon_d^2}{\varepsilon_d + \varepsilon_m}} \tag{10}$$

where λ is the free space wavelength (i.e., $2\pi c/\omega$). Substituting into this expression the relative dielectric constants of air and glass for the leaky and bound modes, respectively, we find good agreement with the FVH-FDM results as shown in Fig. 7.
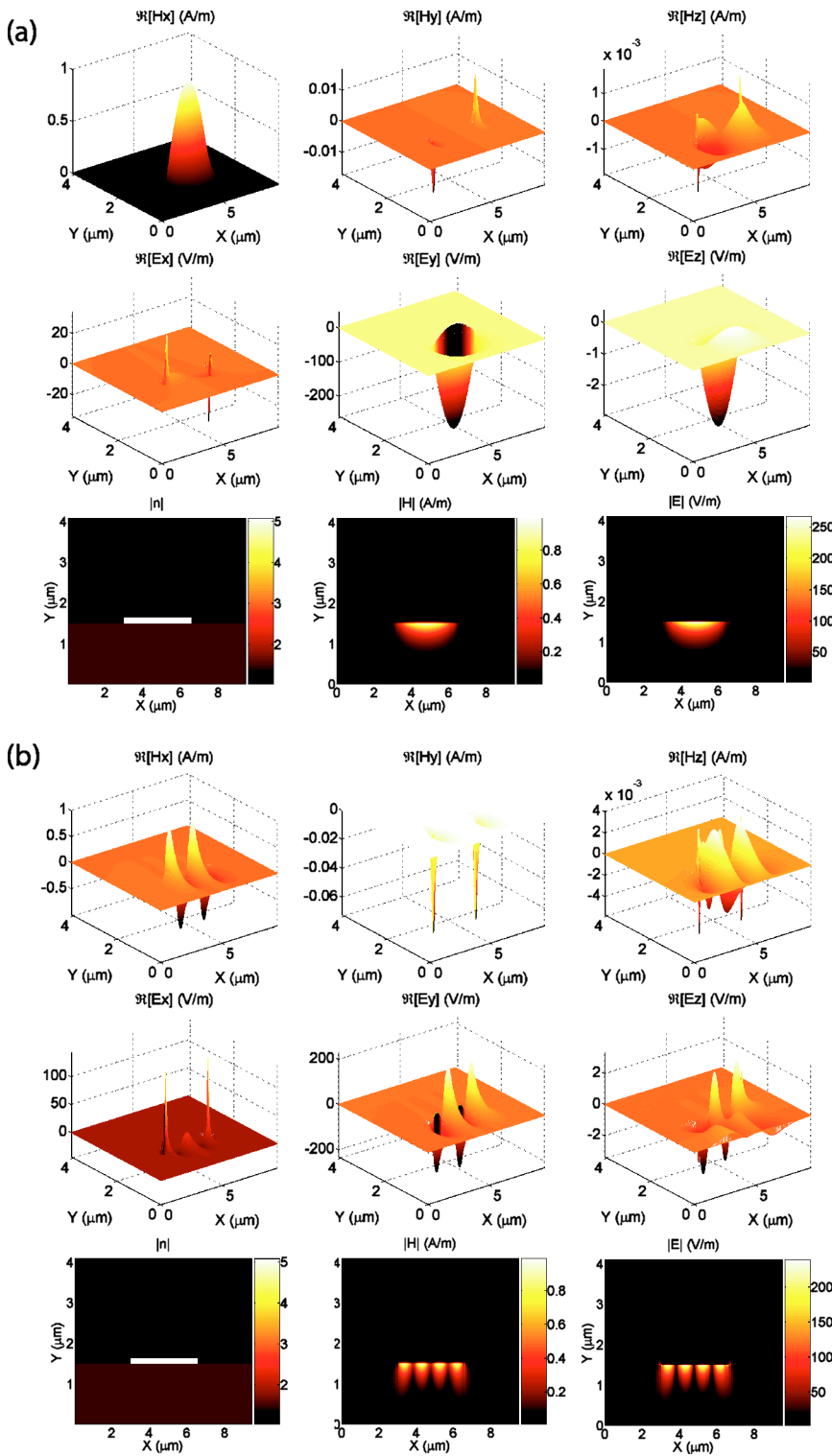
FIG. 4. (Color online) Simulated field profiles for two of the four bound quasi-TM surface plasmon modes of a 3.5 μm wide, 55 nm tall Au stripe waveguide on glass substrate ($\lambda = 800$ nm): (a) lowest order bound mode and (b) fourth order bound mode. Note that these bound modes are localized at bottom glass-metal interface, and were calculated without the use of a PML region. (All fields have been normalized such that $\max|H_x| = 1$ A/m, and the simulated refractive index profile has been provided alongside each mode for reference.)

B. Interpretation of previously reported modal behavior

As anticipated, the behavior of leaky modes as described earlier was also in good agreement with the experimental results presented by Weeber *et al.*[11] The calculated propagation constants for the leaky stripe modes (shown in Fig. 5) are similar to those associated with leaky air-Au SPPs excited along an extended film region (shown in Fig. 2). In contrast, the propagation constants for the bound modes

(shown in Fig. 6) have considerably higher real and imaginary components. The larger imaginary components (α) indicate that the bound modes have greater losses, while the larger real components (β) demonstrate that there is a substantial increase in momentum as compared to the original SPPs in the extended film region. Examining the near-field optical images taken over the launch pad regions where stripe modes are excited, it does not appear that the propa-
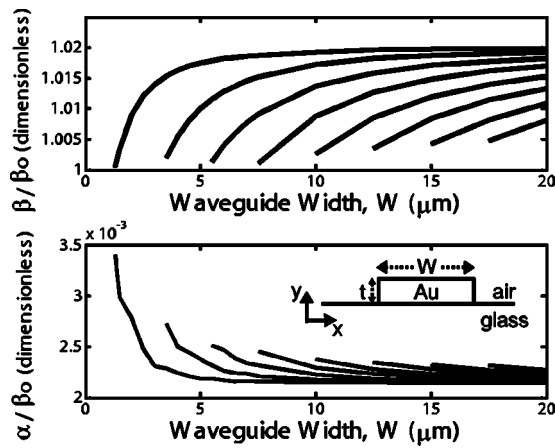
FIG. 5. Complex propagation constants for the eight lowest order leaky, quasi-TM surface plasmon modes of varying width Au stripe waveguides ($t=55$ nm, $\lambda=800$ nm). Inset shows the simulated geometry.

gation constant has changed notably.[29] Neither an appreciable decrease in propagation length due to additional losses nor the horizontal interference patterns characteristic of direct backreflections from a momentum mismatch are easily observed. Therefore, we can find no evidence that the observed modes are bound in nature. In fact, Weeber *et al.* in analyzing their data assume that the propagation constants along both the film region and the metal stripe are equal, and they conclude from this that the SPPs guided by metallic stripes are fundamentally different from those guided by dielectric waveguides. We, however, find that there is an alternative physical interpretation. Based upon our numerical solutions and conventional waveguide theory, we find that the experimental data is consistent with the observation of leaky modes.

To introduce this interpretation, let us first consider the transverse mode profiles from the previously published PSTM studies.[11] For increasing strip widths, it was observed that additional peaks appear in the near-field intensity distributions measured across the waveguides. For example, the
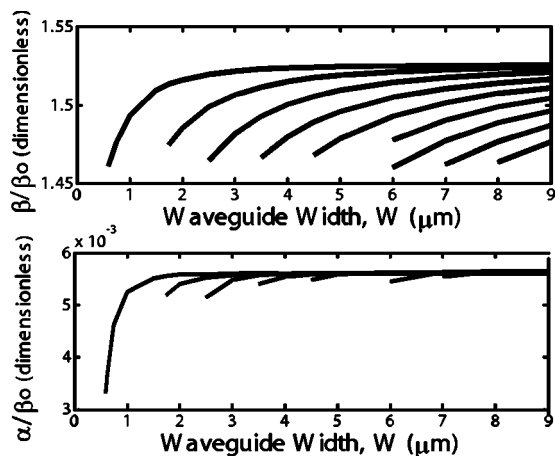

FIG. 6. Complex propagation constants for the nine lowest order bound, quasi-TM surface plasmon modes of varying width Au stripe waveguides ($t=55$ nm, $\lambda=800$ nm).
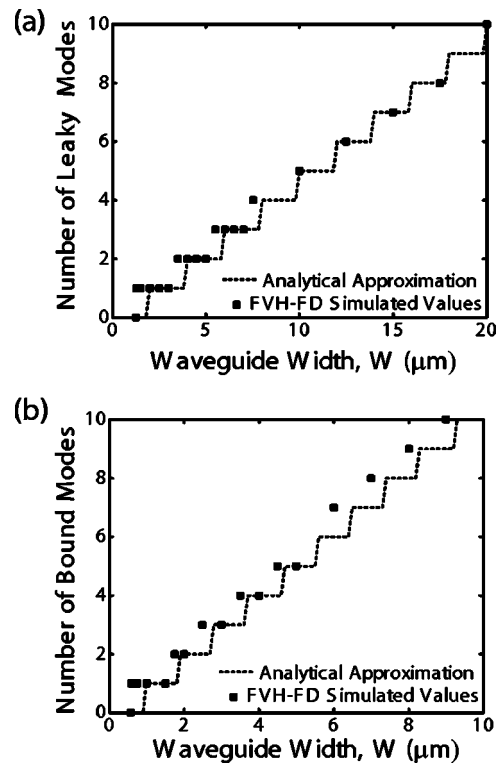

FIG. 7. Comparison with FVH-FDM simulation results for analytical approximation of the number of (a) leaky and (b) bound quasi-TM surface plasmon modes supported as a function of waveguide width.

near-field signal recorded across a 3 μm wide waveguide had three peaks, while the signal of a 3.5 μm wide waveguide had four peaks. Based on our simulation, an additional leaky, quasi-TM mode should become accessible by this 0.5 μm widening, so it is very plausible that the additional peak is related to the introduction of another allowed leaky mode. Yet, given that only one or two modes exist for these waveguides, how does one account for the observation of three or four intensity peaks? While a direct comparison of the simulated modes with recorded near-field intensities would require a thorough understanding of the utilized PSTM, an initial correlation can be made by considering the preferential sensitivity of the utilized near-field probe to particular field components.[30] For this treatment, one must determine the conductivity of the thin chromium layer deposited as a coating on the tapered fiber probe used in Ref. 11. Fortunately, both elemental chromium and chromium oxide, which may form after deposition, do not demonstrate significant ac conductivity at the excitation frequency.[26] Therefore, it is likely that the recorded PSTM image is proportional to the electric field intensity. Figure 8 shows the simulated transverse magnetic field profiles of 1.5, 2.5, and 3.5 μm wide waveguides as well as the electric field intensity at a constant height of 50 nm above the waveguide surface. In addition to the expected maxima between modal nodes in the H_x field, each electric field intensity plot shows two additional peaks associated with dielectric discontinuities at the waveguide edges. For both of the narrower waveguides, only a single leaky quasi-TM mode exists, and the associated
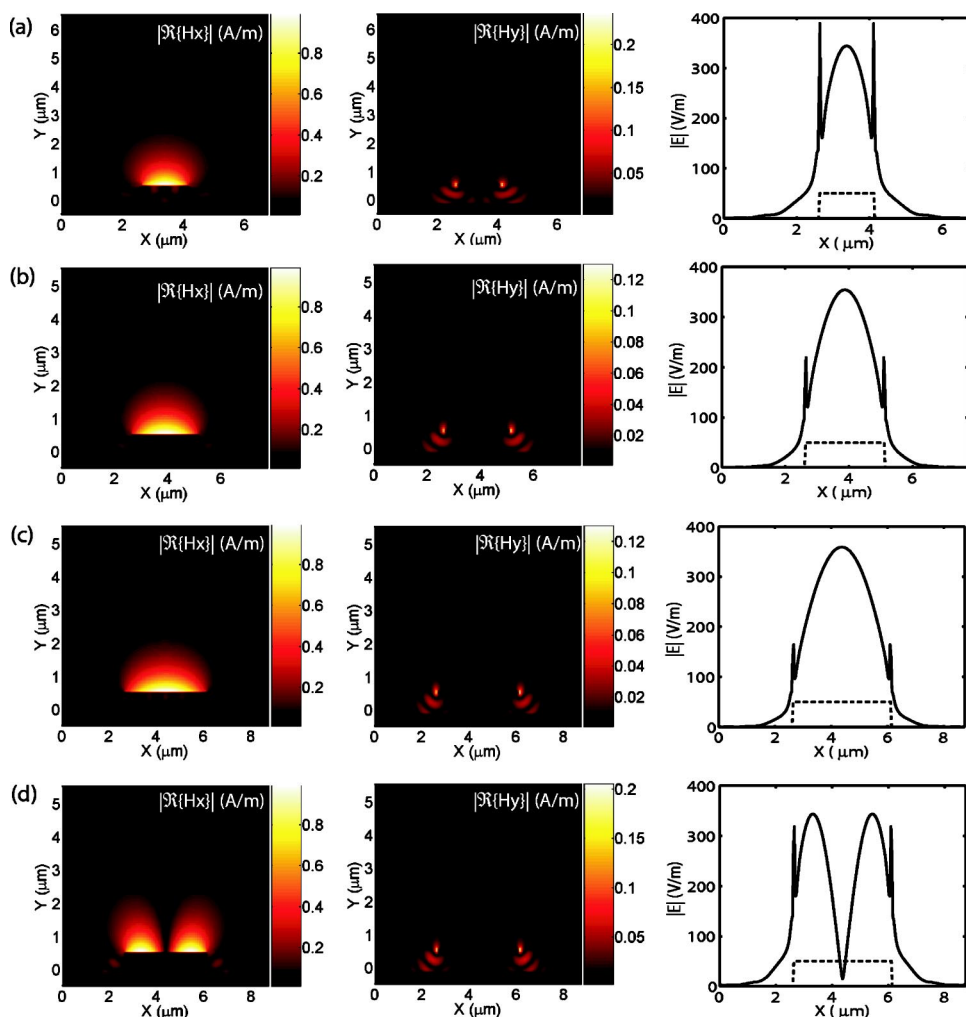
FIG. 8. (Color online) Transverse magnetic field profiles and electric field intensities for leaky, quasi-TM surface plasmon modes of varying width Au stripe waveguides ($t=55$ nm, $\lambda=800$ nm); (a) sole, lowest-order mode for $W=1.5$ μm; (b) sole, lowest-order mode for $W=2.5$ μm; (c) lowest-order mode for $W=3.5$ μm; and (d) second-order mode for $W=3.5$ μm. (Note that the electric field intensity is plotted for a height of 105 nm above the substrate surface, and dashed line denotes location of Au stripe.)

electric field intensity shows three distinct peaks. While for the wider 3.5 μm waveguide, two leaky quasi-TM modes exist, and the associated electric field intensities show four distinct peaks. Comparison with the recorded near-field images from Fig. 3 of Ref. 11 shows that the numbers of simulated peaks exactly match those measured. Despite this agreement in terms of peak number, it should be noted that there are significant differences between the precise location and magnitude of compared peaks. Given the intricacies of near-field microscopy and the myriad of imaging artifacts which can be introduced by sources such as scattered light from surface roughness at the waveguide corners,[31] this initial correlation between numerical simulations and experiment is highly promising.

Our interpretation that multiple peaks in the near-field signal result from the electric field intensities of a single mode also allows for consistent analysis with the well established ray optics interpretation of radiation propagation in waveguides. Such an analytical treatment was originally suggested by Weeber *et al.* However, as they ascribed each intensity peak to the interference of counterpropagating SPP reflections as shown in Fig. 4 of Ref. 11, they concluded that such a view would require a large lateral wave vector comparable to the propagation constants, and thus, many reflections to occur as SPPs traveled down the stripe waveguide.

As the effective reflection coefficient for SPPs at edges can be quite low,[32] Weeber *et al.* concluded that the observed behavior was inconsistent with "standing-wave patterns as in dielectric waveguides." We believe this inconsistency can be resolved by noting that only the central observed peaks, which correspond to maxima in both the electric field intensities and the dominant H_x field of the quasi-TM mode, are a result of interference between counterpropagating reflections. For example, in the 2.5 μm wide waveguide, if only a single peak is ascribed to the standing-wave interference creating the modal H_x field profile shown in Fig. 8, then the lateral wave vector can be approximated to be roughly 1.25 $\times 10^6$ m^{-1} ($k_x \approx \pi/W$). This value is small when compared with the real component of the propagation constant (β) which was simulated as 7.95×10^6 m^{-1}. Given the ratio of these components and the stripe width, one would expect a reflection approximately every 15 μm ($\approx W \times \beta/k_x$) which is consistent with our simulated propagation length of 25.6 μm [$P.L. \approx (2\alpha)^{-1}$]. Similar analysis for the single accessible mode of the 1.5 μm stripe and the higher order mode of the 3.5 μm stripe would anticipate their shorter propagation lengths. Accordingly, it appears that by analyzing the leaky modal solutions of finite width plasmonic waveguides, a self-consistent analytical and numerical interpretation can be formed which helps explain previous experimental results.
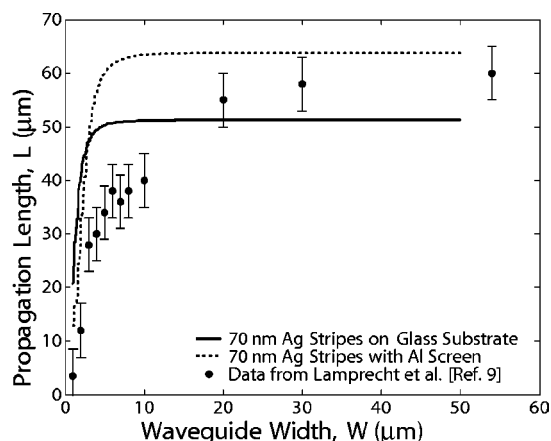
FIG. 9. Comparison of experimental results in Ref. 9 to simulated propagation lengths for lowest-order leaky, quasi-TM surface plasmon modes of varying width Ag stripes ($\varepsilon_{Ag}=-18.3136+0.47941i$) (see Ref. 33) on glass substrate with and without 50 nm silica/50 nm Al screening layer ($\varepsilon_{Al}=-51.314+19.43i$) (see Ref. 26).

Given the pace of experimental results regarding SPPs in recent years, there is no shortage of data with which to compare the numerical simulations of leaky surface plasmon modes. In an early publication on finite width plasmonic waveguides, Lamprecht *et al.* probed the dependence of propagation length on waveguide width.[9] Using far-field microscopy techniques, the authors monitored light scattered by surface roughness from SPPs excited via ATR in a Kretschmann configuration. To differentiate between excitation and propagation regions, a thin Al screening film was used in these experiments, which the authors concluded reduced losses by preventing reradiation into the prism. Based on the sharp decline in propagation length observed with decreasing stripe widths, Lamprecht *et al.* noted that a fundamental change in the propagation constant of SPPs occurs for finite width structures, and their paper suggested that this was a result of increased surface scattering along the lateral stripe edges for narrower waveguides. However, we have simulated the leaky modes of waveguide structures similar to those in Ref. 9, and based purely on the ideal case without scattering losses, the simulated modes show a decrease in propagation length with decreasing stripe width as plotted in Fig. 9. Our results suggest that, while both observations presented by Lamprecht *et al.* are correct, these two phenomena are correlated, not causal. That is, there is both a change in

the modal propagation constant due to finite width, and an increase in losses due to surface scattering at the lateral edges. Moreover, with our numerical treatment, we can quantify the relative contributions of these two separate mechanisms. Note that diminished propagation length in the simulation results only becomes significant for waveguide widths smaller than 5 μm. Thus, for narrower waveguides, it appears that the significant decay in propagation length observed experimentally results from fundamental modal loss (i.e., absorption and radiation losses); whereas for the larger waveguides with widths between 5 and 10 μm, scattering losses likely account for the additional losses. Our simulation results also suggest that experimental use of an Al screening layer introduces an unanticipated dependence on stripe width. This dependence can be seen when comparing simulated propagation lengths for the waveguides with and without the Al screening layer. For wide stripes, the Al region clearly improves propagation length by reducing radiation losses into the prism, but for narrower structures, this layer results in reduced propagation lengths due to additional absorptive losses as the mode begins to extend significantly into this region.

IV. CONCLUSION

Having presented a numerical technique capable of solving for both the bound and leaky modes of plasmonic waveguides, we have shown that leaky modal analysis can provide valuable insight into the experimentally observed behavior of SPP propagation. In particular, simulation results for metallic stripe waveguides highlighted the differences between bound and leaky modes as well as the dependence of modal confinement on waveguide width. A cutoff width was found below which no quasi-TM modes existed, and an analytical model was derived to predict the finite number of allowed modes for these structures. Comparison with published experimental results allowed for reinterpretation of previous measurements in a manner consistent with a ray optics view of waveguide behavior, and demonstrated that numerical simulations can be used to predict practical waveguide characteristics such as propagation length.

*Email address: zia@stanford.edu

[1] W. L. Barnes, A. Dereux, and T. W. Ebbesen, Nature (London) **424**, 824 (2003).

[2] J. Takahara, S. Yamagishi, H. Taki, A. Morimoto, and T. Kobayashi, Opt. Lett. **22**, 475 (1997).

[3] M. Quinten, A. Leitner, J. R. Krenn, and F. R. Aussenegg, Opt. Lett. **23**, 1331 (1998).

[4] J. C. Weeber, A. Dereux, Ch. Girard, J. R. Krenn, and J. P. Gou-

donnet, Phys. Rev. B **60**, 9061 (1999).

[5] M. L. Brongersma, J. W. Hartman, and H. A. Atwater, Phys. Rev. B **62**, R16 356 (2000).

[6] R. Zia, M. D. Selker, P. B. Catrysse, and M. L. Brongersma, J. Opt. Soc. Am. A **21**, 2442 (2004).

[7] J. R. Krenn, B. Lamprecht, H. Ditlbacher, G. Schider, M. Salerno, A. Leitner, and F. R. Aussenegg, Europhys. Lett. **60**, 663 (2002).

[8] J. R. Krenn and J. C. Weeber, Philos. Trans. R. Soc. London, Ser. A **362**, 739 (2004).

[9] B. Lamprecht, J. R. Krenn, G. Schider, H. Ditlbacher, M. Salerno, N. Felidj, A. Leitner, and F. R. Aussenegg, Appl. Phys. Lett. **79**, 51 (2001).

[10] J. C. Weeber, J. R. Krenn, A. Dereux, B. Lamprecht, Y. Lacroute, and J. P. Goudonnet, Phys. Rev. B **64**, 045411 (2001).

[11] J. C. Weeber, Y. Lacroute, and A. Dereux, Phys. Rev. B **68**, 115401 (2003).

[12] G. Schider, J. R. Krenn, A. Hohenau, H. Ditlbacher, A. Leitner, F. R. Aussenegg, W. L. Schaich, I. Puscasu, B. Monacelli, and G. Boreman, Phys. Rev. B **68**, 155427 (2003).

[13] P. Berini, Phys. Rev. B **61**, 10 484 (2000).

[14] P. Berini, Phys. Rev. B **63**, 125417 (2001).

[15] S. J. Al-Bader, IEEE J. Quantum Electron. **40**, 325 (2004).

[16] H. Raether, *Surface Plasmons on Smooth and Rough Surfaces and on Gratings* (Springer-Verlag, Berlin, 1988).

[17] W. P. Chen, G. Ritchie, and E. Burstein, Phys. Rev. Lett. **37**, 993 (1976).

[18] R. Charbonneau, P. Berini, E. Berolo, and E. Lisicka-Shrzek, Opt. Lett. **25**, 844 (2000).

[19] P. Lusse, P. Stuwe, J. Schule, and H. G. Unger, J. Lightwave Technol. **12**, 487 (1994).

[20] W. P. Huang, C. L. Xu, W. Lui, and K. Yokoyama, IEEE Photonics Technol. Lett. **8**, 652 (1996).

[21] W. C. Chew, J. M. Jin, and E. Michielssen, Microwave Opt. Technol. Lett. **15**, 363 (1997).

[22] N. N. Feng, G. R. Zhou, C. Xu, and W. P. Huang, J. Lightwave Technol. **20**, 1976 (2002).

[23] S. S. A. Obayya, B. M. Azizur Rahman, K. T. V. Grattan, and H. A. El-Mikati, J. Lightwave Technol. **20**, 1054 (2002).

[24] G. M. Berry, S. V. Burke, J. M. Heaton, and D. R. Wright, Electron. Lett. **29**, 1941 (1993).

[25] S. Selleri, L. Vincetti, A. Cucinotta, and D. M. Zoboli, Opt. Quantum Electron. **33**, 359 (2001).

[26] E. D. Palik, *Handbook of Optical Constants and Solids* (Academic, Orlando, FL, 1985).

[27] E. Anemogiannis, E. N. Glytsis, and T. K. Gaylord, J. Lightwave Technol. **17**, 929 (1999).

[28] Hermann A. Haus, *Waves and Fields in Optoelectronics* (Prentice-Hall, Englewood Cliffs, NJ, 1984).

[29] For example, see Figs. 6(b) and 8(b) of Ref. 11.

[30] A. Dereux, E. Devaux, J. C. Weeber, J. P. Goudonnet, and C. Girard, J. Microsc. **202**, 320 (2001).

[31] For an illustrative example of scattering at waveguide edges, see Fig. 3(b) in Ref. 9.

[32] H. A. Jamid and S. J. Al-Bader, IEEE Photonics Technol. Lett. **7**, 321 (1995).

[33] P. B. Johnson and R. W. Christy, Phys. Rev. B **6**, 4370 (1972).